



Descaling behaviour of stainless steel following simulated reheating

by P.C. Pistorius*, N.-A. Quagrainie*, and C. Coetzee*

Synopsis

Experimental results are presented that test the hypothesis that the descaling behaviour of stainless steel slabs following reheating is controlled by interfacial roughening at the scale-steel interface. In this investigation, two stainless steels were considered: type 304 (austenitic, with 18% Cr and 8% Ni) and type 412 (ferritic/martensitic, with 11.6% Cr). It was found that the entanglement that arises at the scale-steel interface was in fact effective in maintaining scale-steel adhesion, under the mechanical descaling conditions used. In the case of type 304, descaling proceeded by fracture along chromite layers, which formed (by internal oxidation) on the austenite grain boundaries; for this steel, the extent of descaling depends most strongly on austenite grain structure, and not primarily on the conditions in the reheating furnace. In contrast, type 412 samples descaled only at the edge of the entangled zone, and showed a greater sensitivity to the reheating conditions; specifically, higher free oxygen in the reheating gas and longer reheating times were found to increase the residual scale thickness.

Key words: stainless steel, reheating, scale, entanglement, descaling, fayalite, internal oxidation, grain structure, free oxygen.

Background

Reheating slabs in an oxidising furnace atmosphere is a common step before hot rolling. During reheating, an oxide scale which can be several millimetres thick forms on the slab surface. This scale must be removed before hot rolling to ensure good surface quality of the hot-rolled strip. Scale removal is normally performed with high-pressure water sprays (hydraulic descaling). The work reported here originated from industry observations that complete scale removal is sometimes not achieved in the case of stainless steels.

The guiding hypothesis for this work was that roughening of the scale-steel interface affects descaling; it has been observed for carbon steels that rougher interfaces (presumably yielding stronger keying of the scale to the steel) are associated with thicker residual scale after descaling¹. Several mechanisms can lead to roughening of the

interface and so affect descaling; these mechanisms are briefly reviewed below.

Both carbon steel and stainless steels generally oxidize by a cationic diffusion mechanism². This means that metal ions diffuse through the scale surface to deposit new scale at the outer surface of the scale, leaving vacancies at the scale-steel interface. These vacancies are generally eliminated by climb of the misfit dislocations at the scale-metal interface³. These misfit dislocations are present at the interface because of the epitaxial relationship between the scale and the underlying metal (i.e., with specific crystal planes and crystallographic directions of the scale parallel to those in the underlying metal)⁵⁻⁷. The dislocations are required to accommodate the misfit between the metal and scale lattices. If the process of vacancy elimination is somehow prevented, the vacancies can condense to form voids at the scale-metal interface—roughening that interface. Vacancy elimination can be prevented by the loss of epitaxy between the scale and the metal, which will result if oxidation occurs through one grain into the next.

Given the thick scales that form during reheating, such loss of epitaxy and void formation appear inevitable. Voids may serve as stress raisers, promoting loss of scale adhesion⁶; this may be an explanation for the observation that thinner scales (formed at lower temperatures) on aluminum-killed steels are more difficult to remove by hydraulic descaling⁸. Conversely, because voids interrupt the movement of cations, scale growth slows down above voids², causing the scale-metal interface to become uneven, which might in fact aid adhesion by a mechanical keying action.

Stress within the scale can cause roughening. The oxide scale on most metals is under compressive stress during growth^{2,6}.

* Department of Materials Science and Metallurgical Engineering, University of Pretoria, Pretoria.

© The South African Institute of Mining and Metallurgy, 2003. SA ISSN 0038-223X/3.00 + 0.00. Paper received Jul. 2003; revised paper received Nov. 2003.

Descaling behaviour of stainless steel following simulated reheating

This compressive stress may cause buckling of the oxide scale, contributing to void formation at the interface, and even leading to deformation of the metal itself⁹. However, these effects appear to be much less prevalent if water vapour is present in the atmosphere, both for iron¹⁰ and for iron-chromium alloys¹¹. Water vapour is generally present in the reheating furnace atmosphere as a combustion product of the fuel gas, hence stress was not considered a likely cause of roughening in this work.

Internal oxidation of chromium (which is more reactive than iron) may occur within the steel behind the metal-scale interface, by reaction of chromium with oxygen (dissolved in the iron lattice). The resulting structure is that of oxide particles distributed within the metal grains, with often higher concentrations at grain boundaries (as a result of locally higher diffusion coefficients)^{2,12}. These oxides may themselves be deleterious to the surface quality, and can also lead to further destabilization of the interface. Internal oxidation^{9,13} was observed for simple Fe-Cr alloys exposed to oxygen^{9,13}, and to water vapour^{11,14}.

Alloying elements (such as nickel), which are more noble than iron (and hence accumulate in metallic form at the scale-metal interface), cause the interface to become unstable¹⁵. The resulting structure at the interface is that of tendrils of nickel-rich 'filigree'¹⁶ extending into the scale, with enhanced oxidation at the grain boundaries of the underlying metal. This intergrowth of the scale and metal is termed 'entanglement'¹⁷. As can be expected, the scale on such steels is much more difficult to remove^{1,4,8,18}.

Finally, in silicon-killed steels, silica accumulates at the scale-metal interface during oxidation. FeO and SiO₂ form a eutectic system (with melting point around 1180°C); the eutectic composition is close to fayalite (Fe₂SiO₄). This means that, for reheating temperatures greater than 1180°C, a liquid oxide is present next to the metal; this causes the interface to break down, apparently because the fayalite melt wets and penetrates the grain boundaries of the steel. The resulting interpenetration of scale and metal renders the scale difficult to remove^{4,8,16-22}.

Experimental approach

Two stainless steels were considered—type 304 (austenitic), and type 412 (ferritic-martensitic). The compositions are given in Table I. Hot-rolled and pickled plate samples (10 mm thick) were used. The samples were degreased (with acetone) before scaling.

The experimental arrangement is depicted in Figure 1. The samples (with typical dimensions of 100 mm x 50 mm x 10 mm) were heated in a vertical tube furnace (with an inner bore of 76 mm). Large samples were used to avoid edge effects (where the stress within the scale can cause scale-steel separation at sample corners). The gas that passed through the tube was chosen to simulate the combustion product of methane with air, with 3% or 4% free oxygen. The gas mixture therefore consisted of a mixture of N₂, CO₂, O₂, and H₂O (for example, for the case of 4% free oxygen, the gas composition was 72.9% N₂, 4.0% O₂, 7.7% CO₂ and 15.4% H₂O). The total gas flow rate was 4 Ndm³ per minute, which was selected to give similar mass transfer conditions (which depend on the Reynolds number) to industrial

Table I

Composition (mass percentages) of stainless steel samples

Element	Grade	
	412	304
C	0.021	0.044
S	0.0024	0.0033
P	0.026	0.022
Mn	0.485	1.305
Si	0.72	0.40
V	0.08	0.12
Cu	0.09	0.09
Co	0.02	0.03
Ti	0.034	0.010
Mo	0.02	0.14
Cr	11.62	18.16
Ni	0.34	8.09
Al	0.002	0.004
Nb	0.002	0.003
B	0.003	0.001
N	0.0213	0.050
O	0.0037	0.0080

furnaces²³. The nitrogen, carbon dioxide and oxygen were mixed from the pure gases using rotameters. As shown in Figure 1(a), the water content of the resulting gas was controlled by first passing the gas through a saturator (water near its boiling point) and then through a helical condensor, typically maintained at 55°C, where the excess water was condensed out of the gas. The composition of the mixed gas was checked periodically by analysing the water-free gas with a mass spectrometer, and by passing the water-containing gas through a water-absorbing material ('Drierite') for a set time, measuring the mass increase after a controlled time.

The surface roughness of the samples used here was unchanged from that on the as-received pickled plate (with the exception of the as-cast slab samples, which are mentioned below, which retained the as-cast surface finish). Because of the dominant role of internal oxidation (as described below) initial surface roughness does not affect scale adhesions for these steels under these conditions.

The two reheating variables considered were time and excess oxygen. The reheating temperatures were 1210°C for type 412, and 1250°C for type 304, to be in line with plant practice. The temperature during reheating was generally monitored and controlled by means of the furnace thermocouple. However, in two runs an additional thermocouple was spot-welded to the sample surface, and it was found that the sample temperature was generally within 10°C of the furnace temperature—the samples did not heat significantly above the furnace temperature. Some heating of the samples is expected from the exothermic nature of the oxidation reactions, but this was found not to be significant for these samples.

At the end of the scaling period, the sample was removed from the furnace. Care was taken to remove the sample from the furnace in a rapid and reproducible way, to avoid cooling before descaling. The hot sample was subjected to mechanical descaling by bending the sample in a punch-and-anvil combination, inducing a tensile deformation of approximately 10% on the lower surface of the sample. This procedure is shown schematically in Figure 1(b). The punch

Descaling behaviour of stainless steel following simulated reheating

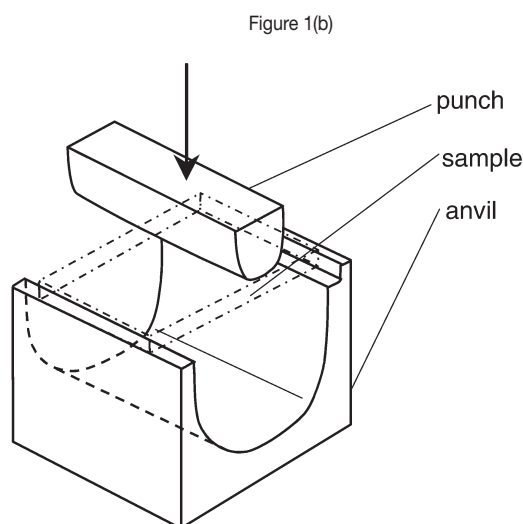
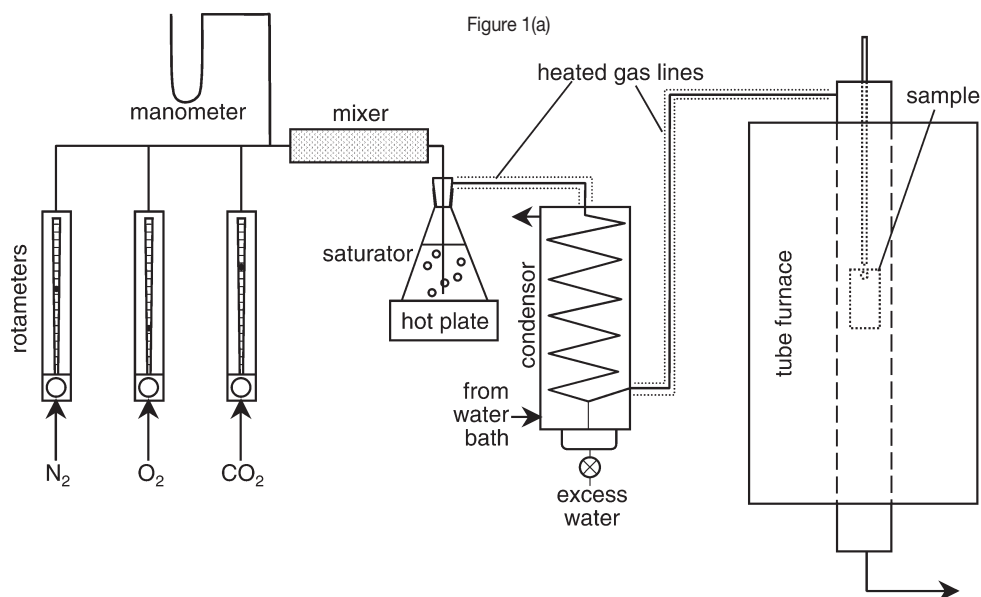


Figure 1—Experimental configuration used to: a) grow scale under simulated reheating furnace conditions, b) mechanically descale sample

was driven by a pneumatic cylinder, which could give a maximum force of 10 kN. The vertical displacement of the punch was controlled by means of limit switches to ensure that the amount of deformation was the same in each case (to yield the same radius of curvature, which was approximately 12 mm).

This approach—mechanical descaling of the hot specimen—is similar to that used by Tuck and Barlow²⁴ and, as in that work, does not claim to simulate exactly the stress conditions during hydraulic descaling. Rather, it is used to give a relative ranking of scale adhesion for different reheating conditions. There is no clarity on the primary mechanism of scale removal during hydraulic descaling, which renders an exact laboratory simulation impossible. However, the choice of bending is based on the observation that the removal mechanism is probably largely mechanical²⁵ (rather than involving significant thermal shock, for example), so the choice of tensile deformation to remove the scale is at least reasonable.

Descaled samples were mounted in resin, and cross-

sections polished for examination by scanning electron microscopy (SEM). Samples were taken from both the deformed (mechanically descaled) and the undeformed (not descaled) regions. The average thickness of scale remaining on the descaled surfaces was found by means of image analysis (of the SEM images). Energy-dispersive X-ray analysis (EDX) was used for point analyses of the various phases.

Results and discussion

Macroscopic appearance of scale

For samples that were not descaled, the scale was several millimetres thick (e.g. about 4 mm after 6 h of scaling for type 412, and about 2 mm for type 304 after the same period). The scale consisted of an inner and an outer layer, similar in thickness. The outer layer consisted largely of iron oxide. The inner layer was largely an iron-chromium spinel (similar in composition to chromite), with other phases close to the scale-steel interface, as discussed below. Platinum wire

Descaling behaviour of stainless steel following simulated reheating

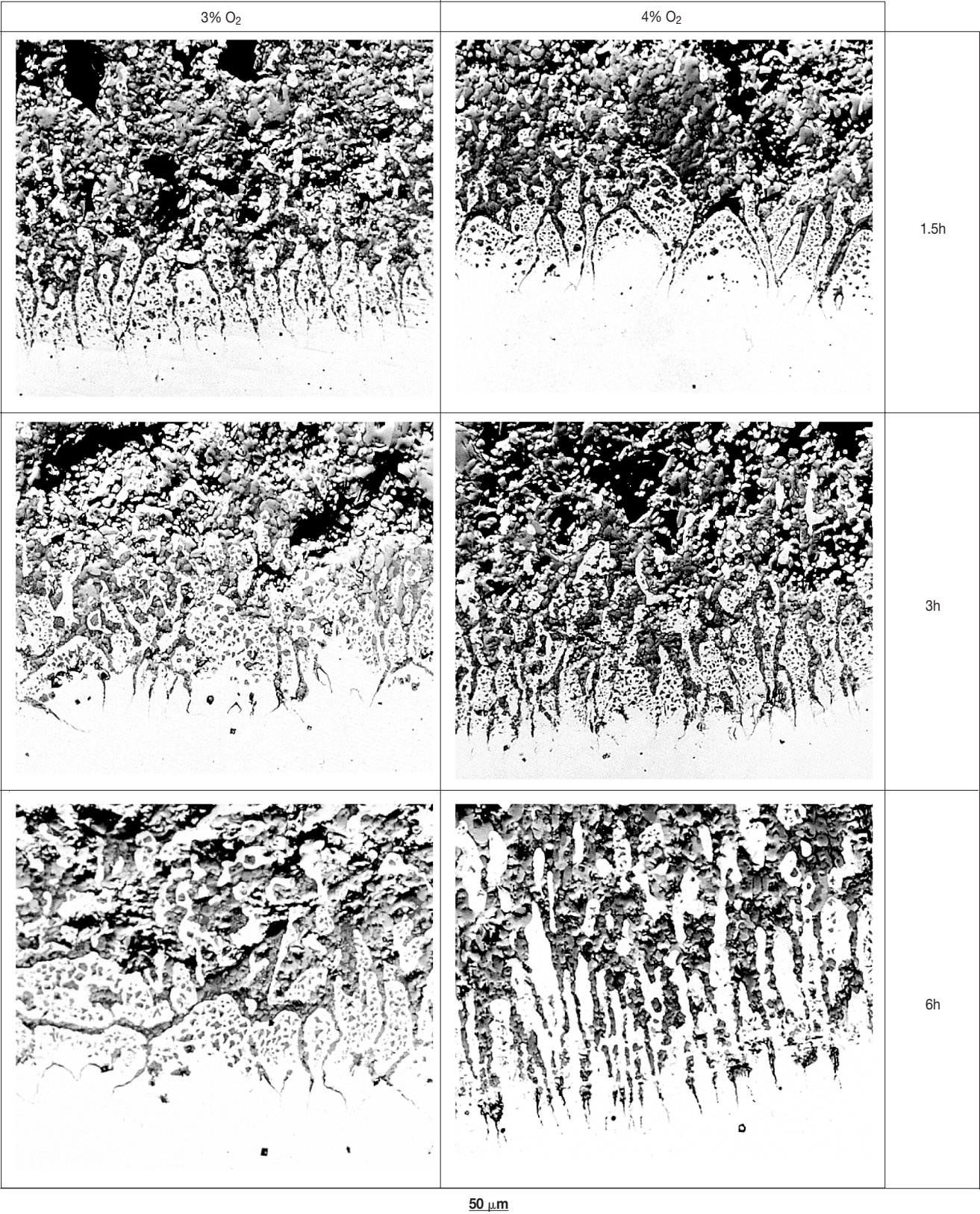


Figure 2—Development of entanglement at the scale-steel interface, for type 412 stainless steel, at a reheating temperature of 1210°C (scanning electron micrographs using back-scattered electrons). In all of the images, the scale is towards the upper part of the image, and the steel substrate towards the bottom. Samples have not been mechanically descaled. Each pair of images is for the same reheating time, but for two different levels of excess oxygen. The reheating time is indicated to the right of each pair of images

Descaling behaviour of stainless steel following simulated reheating

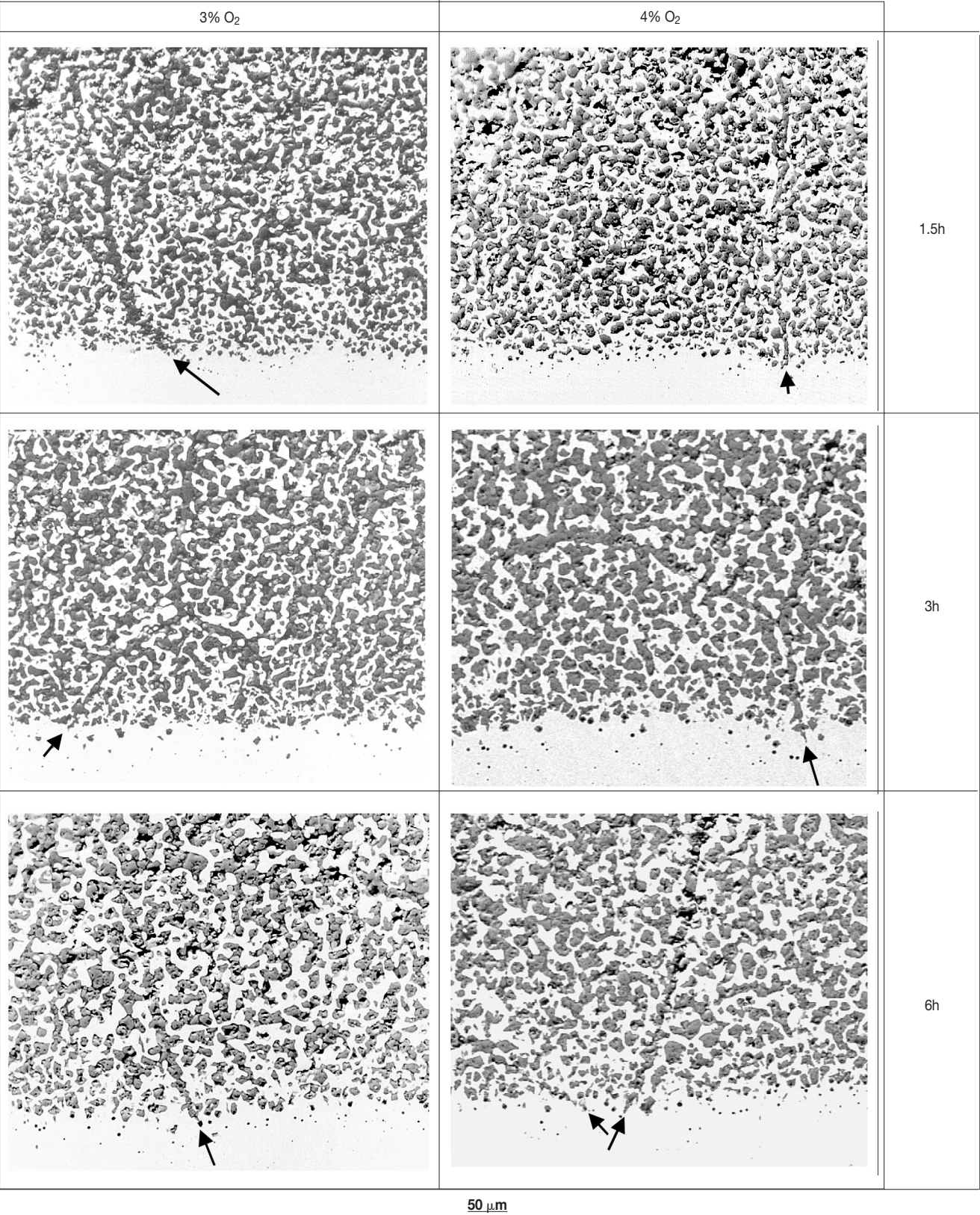


Figure 3—Change in appearance of the scale-steel interface, for type 304 stainless steel, after reheating at 1250°C, without descaling (scanning electron micrographs using back-scattered electrons). In all of the images, the scale is towards the upper part of the image, and the steel substrate towards the bottom. Each pair of images is for the same reheating time, but for two different levels of excess oxygen. The reheating time is indicated to the right of each pair of images. Arrows indicate metal-free chromite regions in the scale

Descaling behaviour of stainless steel following simulated reheating

markers, which were present on the surface of the samples before scaling, were subsequently found at the interface of the two scale layers—illustrating that the outer layer grew by cationic diffusion, but that internal oxidation played a large role in the development of the inner layer. This structure is in good agreement with that found for oxidation of iron-chromium alloys in water vapour¹⁴.

Interfacial roughening

Closer examination of the metal-scale interface revealed severe entanglement, for both type 412 (Figure 2) and type 304 (Figure 3).

Entanglement such as that shown in Figure 2 for type 412 was not reported for binary iron-chromium alloys,¹⁴ despite these being similar to type 412 in chromium content. This indicates that the entanglement in type 412 is related to the presence of residual elements, and closer examination of the entangled region does reveal an effect of silicon. As Table I shows, this steel contained 0.72% Si. Similar to what occurs during scaling of silicon-killed carbon steels, this silicon (once oxidized) accumulates at the scale-metal interface, and forms a fayalite-based oxide melt. During cooling after scaling, this melt solidified to give a eutectic fayalite-wüstite mixture, as shown in Figure 4.

In the case of type 304, tendrils of unoxidized metal were found in the inner scale (see Figure 3), as expected from the high nickel content of this steel. (In this figure, the metal tendrils are visible as the lighter regions entwined with darker oxide in the upper parts of the micrographs.) Close to the steel-metal interface these tendrils typically contained 4–11% chromium and 12–15% nickel (balance iron), with the chromium content decreasing to 3–4% and the nickel content increasing to about 70% in the outer regions of the iron-chromium scale (that is, beneath the outer iron oxide scale). Some narrow paths through the scale were found to be free of the nickel-enriched tendrils (see Figure 3 for examples). These paths—corresponding to chromite in composition—were found to follow the austenite grain boundaries, and extended into the metal beyond the macroscopic scale-steel interface (Figure 3), indicating that these are chromite layers that formed by internal oxidation on the austenite grain boundaries. As discussed later, these chromite paths play an important role in descaling.

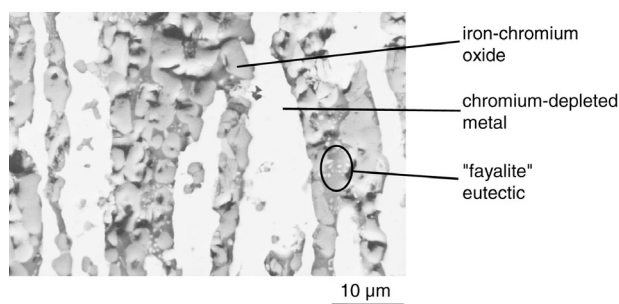


Figure 4—Detail of the phases present in the entangled region for type 412 stainless steel, showing the presence of the fayalite-based eutectic oxide mixture. Scanning electron image using back-scattered electrons. Sample reheated at 1210°C for 6 hours, in an atmosphere containing 4% free oxygen

Thickness of residual scale

Figure 5 shows the measured residual scale thicknesses for the two steel grades. These results show the behaviour of type 412 and type 304 to be quite different—while the former steel grade is quite sensitive to reheating time and excess oxygen (with increases in both elevating the amount of residual scale), this is not the case for type 304. The type 304 samples have nearly constant residual scales of 0.2–0.3 mm thick, for reheating times of 3 and 6 hours, and for both levels of excess oxygen.

These differences (with time, atmosphere and steel grades) arise from differences in the structure of the scale; these differences are apparent in Figures 2 and 3.

Figure 2 illustrates the way in which the width of the entangled region increases with longer reheating times and higher excess oxygen contents, for type 412 steel—in line with the effect of such processing changes on the amount of residual scale (Figure 5). This direct link between the width of the entangled region and the residual scale thickness is illustrated by Figure 6, which shows a lower-magnification image of a sample that had been reheated for 6 hours and then mechanically descaled. Evidently, fracture of the scale occurred at the outer edge of the entangled region, leaving the entire entangled region attached to the steel substrate. The strong effect of reheating conditions on the amount of residual scale has clear implications for the need to control excess oxygen closely in industrial operations.

In contrast, the residual scale thickness on the type 304 samples was not much affected by reheating conditions and, if anything, somewhat decreased for higher excess oxygen and longer reheating. This difference is caused by the way in which the type 304 samples descaled. As Figure 7 illustrates, descaling arose by the formation of numerous cracks through the scale. Closer examination revealed that these cracks followed areas of metal-free scale (chromite layers), such as those arrowed in Figure 3. ('Metal-free scale' here indicates regions of the scale that consisted of oxide only, without any nickel-enriched metal tendrils.) The metal-free chromite scale regions offer low-toughness fracture paths, and so the extent of descaling is linked directly to the prevalence of these fracture paths in the strongly entangled scale; no descaling was observed between the substrate and the scale where such chromite paths were absent. Because chromite layers form on the austenite grain boundaries by internal oxidation, the fracture paths during subsequent descaling depend on the austenite grain structure.

This correspondence between the austenite grain structure and the fracture paths is confirmed by Figure 8, which shows (in Figure 8 a) a cross-sectioned sample which had been etched (using the electrolytic oxalic acid etch) to reveal the austenite grain structure, and (in Figure 8 b) the appearance of the as-descaled surface. The topography visible in Figure 8 b is that of the residual scale attached to the stainless steel sample. The cracks through this residual scale can be seen to delineate a typical austenitic grain structure.

The effect of austenite grain structure on descaling implies that the microstructure of the as-cast slab assumes an unexpected importance in descaling – if the extent of scale growth is such that the chill zone is fully oxidised, and the scale grows into columnar zone, descaling is likely to be much poorer (and the extent of slab grinding is of course relevant to this). This indirect effect may well account for

Descaling behaviour of stainless steel following simulated reheating

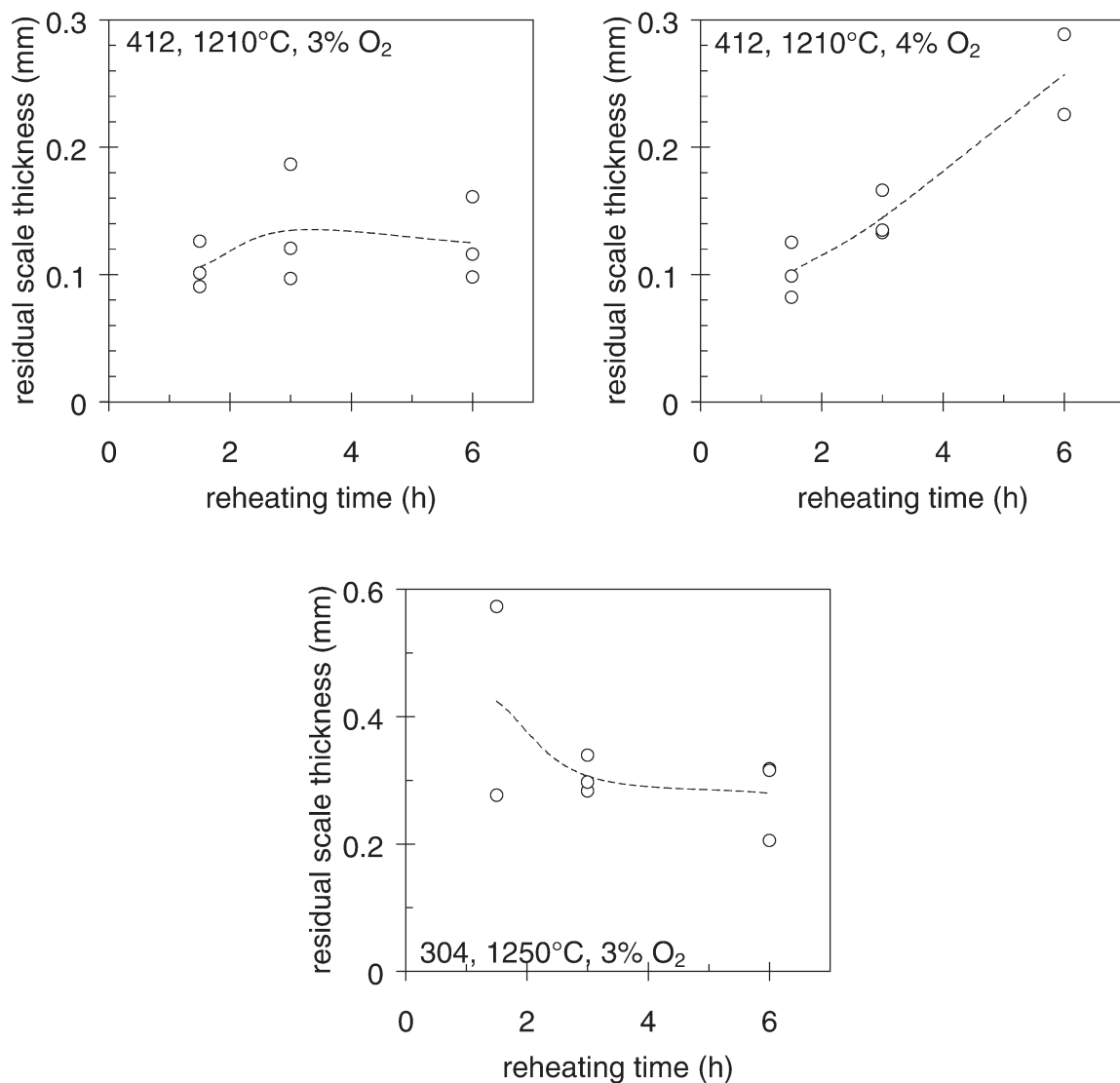


Figure 5—Measured residual scale thickness, for type 412 and type 304 samples, reheated at respectively 1210°C and 1250°C, for varying times, and with 3% and 4% free oxygen in the furnace atmosphere. The data points show measurements at three positions on each descaled surface, and the broken line the average of these measurements

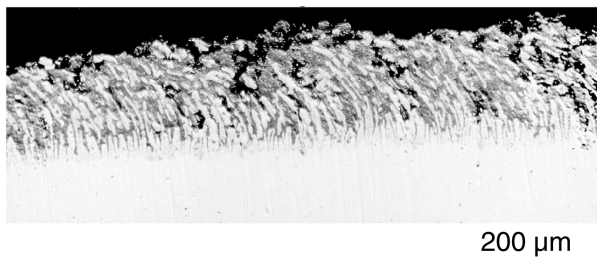


Figure 6—Residual scale on a type 412 sample, after descaling following reheating for 6 hours at 1210°C in an atmosphere containing 4% free oxygen (the scale is towards the upper part of the image, and the steel substrate towards the bottom). Scanning electron image using back-scattered electrons. Comparison with Figure 2 shows that the residual scale thickness corresponds to the full thickness of the entangled region

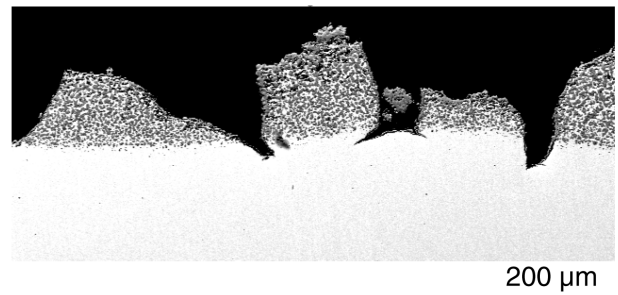
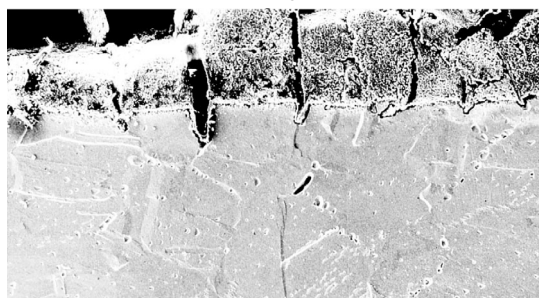


Figure 7—Residual scale on a type 304 sample, after descaling following reheating for 6 hours at 1250°C in an atmosphere containing 4% free oxygen (the scale is towards the upper part of the image, and the steel substrate towards the bottom). Scanning electron image using back-scattered electrons

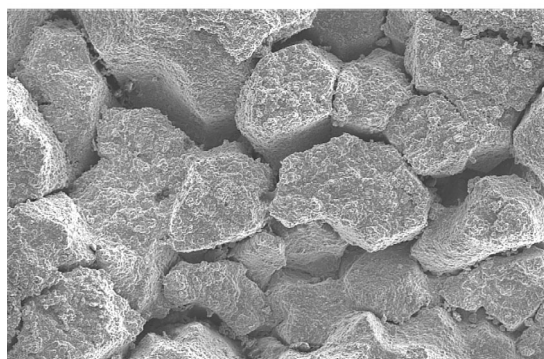
Descaling behaviour of stainless steel following simulated reheating

Figure 8 a)



200 μ m

Figure 8 b)



200 μ m

Figure 8—Correspondence between the crack paths through the scale on reheated type 304 and the austenite grain structure.

a) Etched cross-section of a type 304 samples reheated for 6 hours at 1250°C. The sample was electrolytically etched in oxalic acid to reveal the microstructure of the steel. Cracks in the residual scale can be seen to correspond to grain boundaries in the underlying steel microstructure. Secondary electron image.

b) Appearance of the exterior surface of a descaled type 304 sample, showing that the appearance of the cracked residual scale reflects the underlying austenite grain structure. Secondary electron image

much of the variability in descaling behaviour which is observed practically. To test this idea, slab samples of type 304 stainless steel were obtained, and reheated in the same way. The samples were of two different kinds: one where the original as-cast surface was intact, and one where the surface of the slab had been ground into the columnar zone (as is often done to remove superficial defects). Figure 9 illustrates that the grain structure (especially grain shape) of these samples close to their surfaces were quite different—the more equiaxed grains of the chill zone (as-cast sample) contrast with the columnar grains of the ground sample. The columnar grains predominantly have grain boundaries perpendicular to the sample surface, which means that difficulties with descaling are expected.

The scale thickness following reheating was similar for the two kinds of sample, as shown by Figure 10. However, upon descaling large differences are apparent. As Figure 11 reveals, the residual scale on the ground sample is much thicker than on the as-cast sample; the columnar austenite grain structure is transferred to the large thickness of residual scale on the ground sample. These results confirm the importance of grain structure for descaling behaviour of type 304 stainless steel.

Figure 9 a)

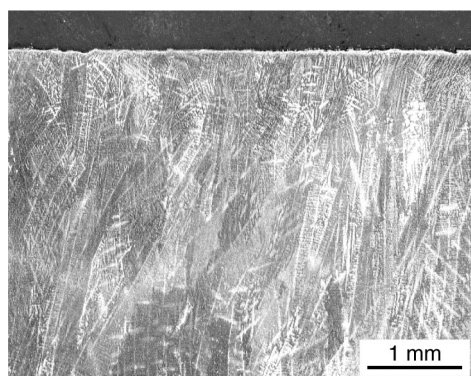


Figure 9 b)

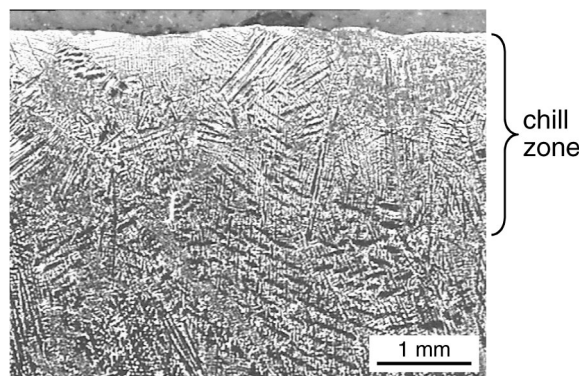


Figure 9—Microstructures of type 304 slab samples, viewed in cross-section, with the free surface at the top. Samples etched electrolytically in dilute nitric acid. a) Ground slab sample b) As-cast slab sample

Figure 10 a)

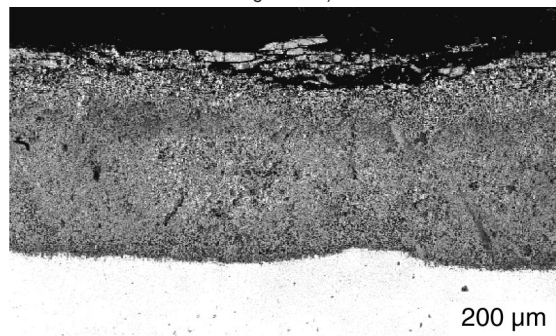


Figure 10 b)

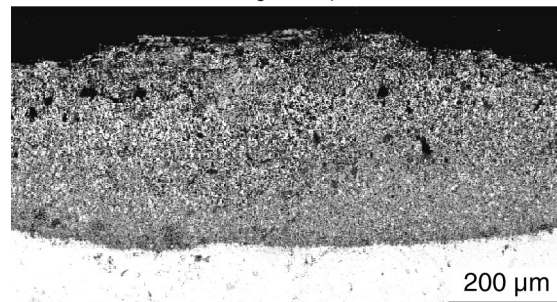


Figure 10—Scale on type 304 slab samples, not descaled, following reheating for 4 hours at 1230°C in an atmosphere containing 4% free oxygen (the scale is towards the upper part of the image, and the steel substrate towards the bottom). Scanning electron image using back-scattered electrons. Not descaled. a) Ground slab sample b) As-cast slab sample

Descaling behaviour of stainless steel following simulated reheating

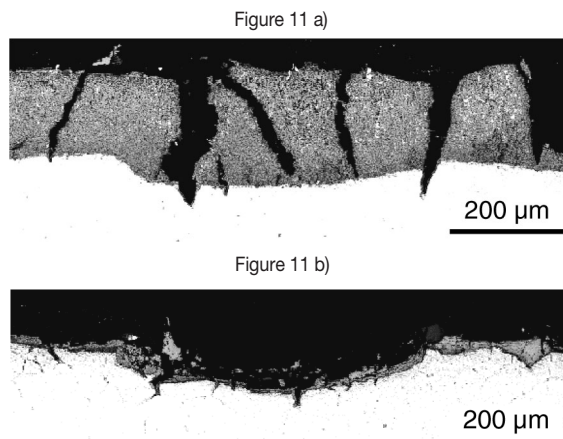


Figure 11—Differences in residual scale on type 304 slab samples which were descaled following reheating for 4 hours at 1230°C in an atmosphere containing 4% free oxygen (the scale is towards the upper part of the image, and the steel substrate towards the bottom). Scanning electron image using back-scattered electrons.

- a) Ground slab sample
b) As-cast slab sample

Conclusions

Of the mechanisms reviewed here, it appears that three contribute to interfacial roughening in these steels: internal oxidation (both type 304 and type 412), fayalite formation (type 412), and 'filigree' formation due to nickel (type 304).

However, the experimental results presented here show that the original hypothesis—that descaling is simply linked to the degree of interfacial roughening—does not fully explain the differences between steel grades and processing conditions. Rather, descaling depends on the presence of metal-free fracture paths through the scale. In the case of type 412, these fracture paths lie at the outer edge of the entangled region (where the metallic fingers have been oxidized). For type 304, the fracture paths follow the austenite grain boundaries (as a result of the formation of chromite layers at the grain boundaries, by internal oxidation).

This difference in behaviour suggests different approaches to favouring descaling in industrial operations. For type 412 (and, by extension other nickel-free ferritic and martensitic grades) the amount of oxidation must be limited—by controlling the excess oxygen and the reheating time. For type 304, longer oxidation in more oxygen-rich atmospheres apparently favours descaling, presumably because this allows more complete development of the chromite layers in the scale.

Control of the austenite grain structure is thus likely to have a strong effect on descaling for nickel-bearing stainless steel grades; small amounts of delta ferrite may serve to pin the austenite grain boundaries and so favour descaling (delta ferrite appears upon reheating at high temperatures, increasing in extent up to the melting point). Also, samples that have been ground (or oxidized) through the chill zone are expected to have thicker residual scales.

Acknowledgements

The research was made possible by support of the Center of Iron and Steelmaking Research at Carnegie Mellon University, Columbus Stainless, Iscor, the Technology and

Human Resources for Industry Programme (THRIP) managed by the National Research Foundation (NRF) and financed by the dti. This material is based on work supported by the National Research Foundation under grant number 2053355.

References

1. ASAI, T., SOSHIRODA, T. and MIYAHARA, M. Influence of nickel impurity in steel on the removability of primary scale in hydraulic descaling. *ISIJ Int.*, vol. 37, 1997. pp. 272–277.
2. P. KOFSTAD. *High temperature corrosion*, Elsevier, London, 1988. pp. 109, 396.
3. RAPP, R.A. Fundamental aspects of high-temperature corrosion. *Journal de Physique*, Colloque C9 3, 1993. pp. 1–15.
4. BOGGS, W.E. The role of structural and compositional factors in the oxidation of iron and iron-based alloys. *Proc. symp. on High temperature gas-metal reactions in mixed environments*. Metallurgical Society of the AIME, New York, 1973. pp. 84–128.
5. RAPP, R.A. The High-Temperature Oxidation of Metals Forming Cation-Diffusing Scales: *Metal. Trans.*, vol. 15A, 1984. pp. 765–782.
6. TANIGUCHI, S. Stresses developed during the oxidation of metals and alloys. *Trans. ISIJ*, vol. 25, 1985. pp. 3–13.
7. PIERAGGI, B. and RAPP, R.A. Stress generation and vacancy annihilation during scale growth limited by cation-vacancy diffusion. *Acta metal.*, vol. 36, 1988. pp. 1281–1289.
8. MORRIS, P., BAGSHAW, P. and MARSTON, H.: *Descaling of steel in rolling mills*. Report EUR 15836, ECSC agreement no. 7210.EA/818, European Commission, Technical Steel Research, Office for Official Publications of the European Communities, Luxembourg. 1996.
9. WHITTLE, D.P. and WOOD, G.C. Complex scale formation on an iron-18 per cent chromium alloy. *J. Electrochem. Soc.*, vol. 114, 1967. pp. 986–991.
10. TUCK, C.W., ODGERS, M. and SACHS, K. The oxidation of iron at 950 C in oxygen/water vapour mixtures. *Corros. Sci.*, vol. 9, 1969. pp. 271–285.
11. FUJII, C.T. and MEUSSNER, R.A. The mechanism of high-temperature oxidation of iron-chromium alloys in water vapor. *J. Electrochem. Soc.*, vol. 111, 1964. pp. 1215–1221.
12. DOUGLASS, D.L. A critique of internal oxidation in alloys during the post-Wagner era. *Oxid. Metals*, vol. 44, 1995. pp. 81–111.
13. WOOD, G.C. and WHITTLE, D.P. The mechanism of breakthrough of protective chromium oxide scales on Fe-Cr alloys. *Corros. Sci.* vol. 7, 1967. pp. 763–782.
14. FUJII, C.T. and MEUSSNER, R.A. Oxide structures produced on iron-chromium alloys by a dissociative mechanism. *J. Electrochem. Soc.*, vol. 110, 1963. pp. 1195–1204.
15. MALDY, J. Sur la structure de l'interface fer-oxyde de fer. Rôle des impuretés résiduelles. *Mémoires Scientifiques de la Revue de Métallurgie*, vol. 62, 1965. pp. 379–398.
16. ZITTERMANN, J.A. BACCO, R.P. and BOGGS, W.E. Factors affecting scale adhesion on steel forgings. *J. Metals*, vol. 34, no. 4, 1982. pp. 22–26.
17. SACHS, K. and TUCK, C.W. Surface oxidation of steel in industrial furnaces. *Proc. conf. Reheating for hot working*, The Iron and Steel Institute, London, 1968. pp 1–17.
18. SHERIDAN, A.T. and SIMON, P. Descaling of steels in rolling mills. *European Steelmaking Developments and Perspectives in Rolling and Reheating*, Commission of the European Communities, Luxembourg, 1995. pp. 233–244.
19. Fukutsuka, T., Nakamura, T., Sato, M., Kokubo, I. and Ishida, R. Study of descaling of steel slabs before hot rolling. *Trans. ISIJ*, vol. 21, 1981. pp. 699–707.
20. Pickens, J.W. The microstructural characteristics of oxide scale formed during bar processing. *21st Mechanical Working & Steel Processing Conference*, Iron and Steel Society/AIME, Warrendale, PA, USA, 1984. pp. 39–65.
21. FUKUGAWA, T., OKADA, H. and MAEHARA, Y. Mechanism of red scale defect formation in Si-added hot-rolled steel sheets. *ISIJ Int.*, vol. 34, 1994. pp. 906–911.
22. PALIN, G.M. Effect of heating conditions on the adhesion of the scale to the metal. *Stal in English*, vol. 8, 1965. pp. 677–679.
23. ABULUWEFA, H.T., GUTHRIE, R.I.L. and AJERSCH, F. Oxidation of low carbon steel in multicomponent gases: Part I. Reaction mechanisms during isothermal oxidation. *Metal. Mater. Trans.* vol. 28A. 1997. pp. 1633–1641.
24. TUCK, C.W. and BARLOW, J. The effect of reheating furnace atmosphere on the adhesion of scale to steel. *Iron and Steel*, vol. 45, 1972. pp. 31–38.
25. BLAZEVIC, D.T. Rolled in scale—the consistent problem. *Proc. of the 4th Int. Steel Rolling Conf.*, Vol. 1. Association de la Siderurgie Francaise, Paris, 1987. pp. A38.1–13. ♦

